SBAS and GBAS Integrity for Non-Aviation Users: Moving Away from "Specific Risk"

Sam Pullen, Todd Walter, and Per Enge
Stanford University

ABSTRACT

SBAS and GBAS enhance standalone GNSS navigation to meet the safety and availability requirements of civil aviation. SBAS and GBAS are also freely available to other users, such as automobiles, buses, and trains on land as well as ships near shore. However, integrity as implemented there are significant differences between the aviation interpretation of navigation integrity and the one that would be natural to most users. This paper explains the differences between "specific risk" as defined by aviation and "average risk," which is used in most other fields and which is the foundation of Probabilistic Risk Assessment (PRA). Maximum errors for the FAA WAAS version of SBAS are presented and compared to the protection levels determined from WAAS to support aviation approach operations to illustrate the degree of conservatism that is built into the "specific risk" interpretation of integrity. Based on this information, several means are proposed to remove this conservatism from SBAS and GBAS for non-aviation users who do not need it. The resulting benefits, in terms of smaller error bounds and/or improved availability, can be substantial.

1.0 INTRODUCTION

Both Space Based and Ground Based Augmentation Systems (SBAS and GBAS, respectively) are designed to enhance standalone GNSS navigation to meet the requirements of civil aviation. SBAS and GBAS corrections and integrity information are also available to the non-aviation user population, such as automobiles, buses, and trains on land as well as ships near shore. This much larger user base can benefit as much from the integrity components of SBAS and GBAS as from the increased accuracy obtained from applying SBAS and GBAS pseudorange corrections. However, there are significant differences between the aviation interpretation of navigation integrity and the interpretation that would be natural to most users.

SBAS and GBAS provide integrity in a multi-step procedure that is laid out in the RTCA *Minimum Operational Performance Standards* (MOPS) for the FAA versions of both systems: DO-229D for the Wide Area Augmentation System (WAAS) [1] and DO-253C for the Local Area Augmentation System (LAAS) [2]. These systems indicate which ranging measurements should be excluded as unsafe to use and provide bounding error standard deviations, or "sigmas," for the remaining usable measurements. Each aircraft uses this information to compute vertical and horizontal protection levels that define position-domain error bounds that can be protected to the desired probability. This process is straightforward, logical, and is not limited to aviation users. However, the requirements and assumptions underlying it make it very conservative.

SBAS and GBAS are designed to meet integrity requirements defined in terms of what is known as "specific risk." Briefly, this means that all safety requirements must be met for the worst combination of knowable or potentially foreseeable circumstances under which an operation may be conducted (see [3]). Some variable factors important to safety, such as the user's satellite geometry, are known by definition. Others, such as receiver thermal noise, are random and unpredictable once the received signal strength is known. But several factors that are critical to GNSS performance, such as multipath and ionospheric errors, are neither completely random nor deterministic. "Specific risk" treats all error sources that are not completely random in a worst-case manner. SBAS and GBAS are designed to mitigate specific risk to support civil aviation, and the resulting conservatism makes SBAS and GBAS less attractive to non-aviation users who expect tighter protection levels relative to nominal system accuracy.

Fortunately, non-aviation users need not apply the MOPS procedures required of aviation users if their own safety requirements are defined differently. Most non-aviation users define integrity in "average" or "ensemble" terms, meaning that everything not known in practice is treated as random and is probabilistically convolved together. The protection levels valid for these users would be much lower than for aviation users, even though the stated bounding probability is the same. This contrast is illustrated in Figure 1, which shows bounds on 2-D horizontal errors at a probability of 0.95 (the 95th percentile, or 95%) for accuracy and a probability of

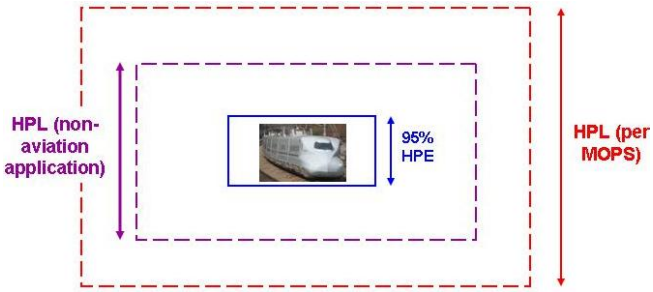

Figure 1: Illustration of 95% Accuracy Bounds and $1 - 10^{-7}$ Protection Levels

$1 - 10^{-7}$ for integrity. The term HPE stands for "Horizontal Position Error," while HPL stands for "Horizontal Protection Level." Analogous terms (VPE and VPL) and a similar picture exist for the vertical dimension.

Only one 95% error bound is shown in Figure 1 because this probability can be observed, estimated, and modeled with theory and reasonable amounts of data on the order of hundreds or thousands of independent samples. Thus, while 95% error bounds will differ among users and environments, they will not differ much because of uncertainty. This is not at all the case at the very small probability of 10^{-7} that applies to aviation precision approach and is roughly equivalent to one event in 47.5 years per 150-second precision-approach interval. Both theory and data fall far short of being able to predict such rare-event errors. Extrapolating from available data to $1 - 10^{-7}$ using Gaussian distributions is fraught with peril because the Gaussian distribution almost never applies at such small probabilities [4,5]. Mixed-Gaussian models, other "fat-tailed" distributions, and inflation of Gaussian parameters help address this, but the uncertainty regarding the true error distribution results in different error bounds depending on the assumptions that are made. The same is true regarding the effects of faults and anomalies that are more probable than 10^{-7} but are still rare and poorly understood.

In the end, different means of assessing these uncertainties and various degrees of user risk aversion result in different $1 - 10^{-7}$ protection levels, as shown in Figure 1. It is this difference that we wish to quantify and exploit in this paper. Section 2.0 defines the "specific risk" approach used in aviation integrity, describe how it is unique to aviation, and explain why it produces larger protection levels (i.e., the "MOPS HPL") than the "average risk" approach that is most common in other applications. An example of how WAAS and LAAS handle rare but extreme ionospheric spatial decorrelation is provided to illustrate how specific risk can lead to much more conservative error bounds than the more common approach of risk averaging. Section 3.0, the heart of this paper, examines the difference between WAAS protection levels and the maximum vertical and horizontal position errors observed by the WAAS Performance Analysis Network (PAN) operated by the William J. Hughes FAA Technical Center (FAATC). Section 4.0 uses these results to propose means of removing specific risk conservatism from SBAS and GBAS protection levels for applications that would benefit from integrity bounds based on average risk. Because some transportation users may wish to combine features of specific and average risk, Section 5.0 explains how this can be done and how the resulting flexibility should support almost all classes of safety-critical applications.

2.0 "AVERAGE" VS. "SPECIFIC" RISK

2.1 Explanation of "Average Risk"

Because the concept of "average" or "ensemble" risk is more intuitive to those with a background in probability, and because it is one of the key principles of Probabilistic Risk Assessment (PRA) [4,7], it helps to define it first before exploring the unique properties of "specific risk." The following definition is the authors' own and has no official provenance:

> ***Average risk*** *is the probability of unsafe conditions based upon the convolved ("averaged") estimated probabilities of all unknown events.*

More specifically, probability distributions are derived (best on the best available knowledge) for all unknown parameters relevant to user safety, and these are combined by probabilistic convolution to create an overall distribution that represents safety risk as a function of the known parameters. While combining multiple complex uncertainty models is non-trivial, Monte Carlo simulation using today's fast computers makes this straightforward except where extremely small probabilities (e.g., 10^{-9} and below) must be represented.

This straightforward, natural interpretation of probability and uncertainty has a major advantage for PRA and decision making under uncertainty in that it cleanly separates the probabilistic calculation of safety risk from the users' and decision makers' *aversion* to risk [8]. A simple version of risk aversion can be illustrated by asking individuals how much money they would be willing to risk in exchange for a 50-50 chance (e.g., a fair coin flip) chance of winning US $10,000. A *risk-neutral* individual, one who has no aversion to a one-shot gamble for significant stakes (or one who is so wealthy that $10,000 is a trivial amount) would be willing to risk $5000 in exchange for this opportunity, but most people would be willing to lose significantly less. In other words, they are *risk averse*. When loss of life is possible, extreme risk aversion is normal and expected, but it must be finite, as a non-zero mortality risk exists for any

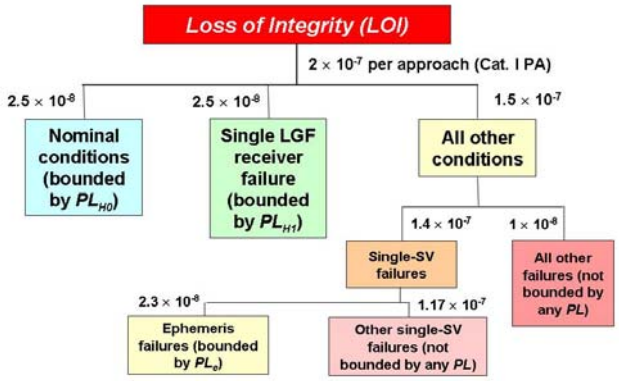

Figure 2: Fault Tree for CAT I GBAS Integrity

activity. However risk aversion is measured, keeping it separate from the actual calculation of risk is very helpful to making logical decisions in the face of uncertainty.

By keeping risk probability and risk severity separate, a final "risk consequence" measure can be derived that allows simplified mathematical manipulation. One useful result of this is known as the *Value of Information* (VOI) [9]. By comparing the risk outcomes of two scenarios in which the latter case has additional information (for example, from an additional sensor or integrity monitor), the risk-reduction benefit of the added information can be traded off against the cost and complexity that it introduces to the system. Similar comparisons can be made for any definition of risk, but the definition and use of VOI in an "average risk" framework makes the most sense in both theory and practice.

2.2 Explanation of "Specific Risk"

To the authors' knowledge, no single comprehensive definition of "specific risk" exists within the aviation safety community. This is partially because of the uniqueness and complexity of the concept and partially because multiple inconsistent interpretations appear to exist. Therefore, the authors again provide their own simplified definition:

> ***Specific risk*** *is the probability of unsafe conditions subject to the assumption that all credible unknown events that could be known occur with a probability of one (on an individual basis).*

To understand how specific risk differs from average risk, it helps to start with a "fault tree" representation of risk in which loss of integrity (LOI) can result from any of the "nodes" of the tree. Figure 2 shows a simplified example of a fault tree for CAT I GBAS [10]. It shows the allocation of the CAT I total integrity risk requirement of 2×10^{-7} per approach to the various possible causes of integrity loss [11]. While fault trees are commonly used with PRA and average-risk analyses, the intent here is to place "sub-allocated" integrity-risk requirements on individual sources of risk and to evaluate each risk separately rather than in combination.

In specific-risk analysis, each type of failure shown in the tree, if deemed to be a "credible" failure (meaning that its assumed prior probability is significant compared to its allocation in the fault tree), is assessed assuming that the failure is guaranteed to occur in a "worst-case" fashion, meaning that the variables that describe the particular fault scenario take the values that maximize the hazard to users. In an average-risk analysis, these variables would take many values according to their own probability distributions, and these distributions would be convolved together to provide an overall representation of risk under this scenario. Instead, one scenario dominates for specific risk, and it is the worst one possible from the system user's standpoint. The improbability of the worst case combination of parameters is not considered as long as the probability of the fault class as a whole is deemed high enough to be of concern.

Since GNSS augmentation systems contain multiple levels of health monitoring, the worst-case scenario is the one that maximizes the probability of an undetected hazardous error. "Hazardous error" is typically defined in simple terms as any error that exceeds a pre-defined safety zone known as an alert limit (AL) or any error that exceeds the computed protection level (PL), which allows integrity to be defined separately from the intended application. Both definitions are conservative in that all errors exceeding AL or PL are treated as equally hazardous; e.g., an error just above AL is treated as just as dangerous as an error of 10 × AL. They are also misleading when used in specific-risk analyses because the resulting "worst-case" conditions are those that give errors just above AL or PL, as these are the hardest for monitor algorithms to detect (see [12]).

This fixation on very improbable worst-case events is foreign to probabilistic risk analysis, but it was not created arbitrarily. The use of specific risk in aviation is an evolution of deterministic guidelines for tolerable risk that go back decades. The airworthiness criteria that apply to CAT III precision landings under Instrument Flight rules (IFR) are documented in FAA Advisory Circular (AC) 120-28D [13], published in 1999, which supersedes earlier versions in 1984 and 1971. They define a probabilistic nominal requirement for landing within a defined "touchdown box" with a probability of $1 - 10^{-6}$, but when faults occur, the requirements cite probability constraints on the worst-case results [13,14].

The specific-risk approach remains dominant in aviation safety assessment because it is partly responsible for the development of safe and reliable air transportation

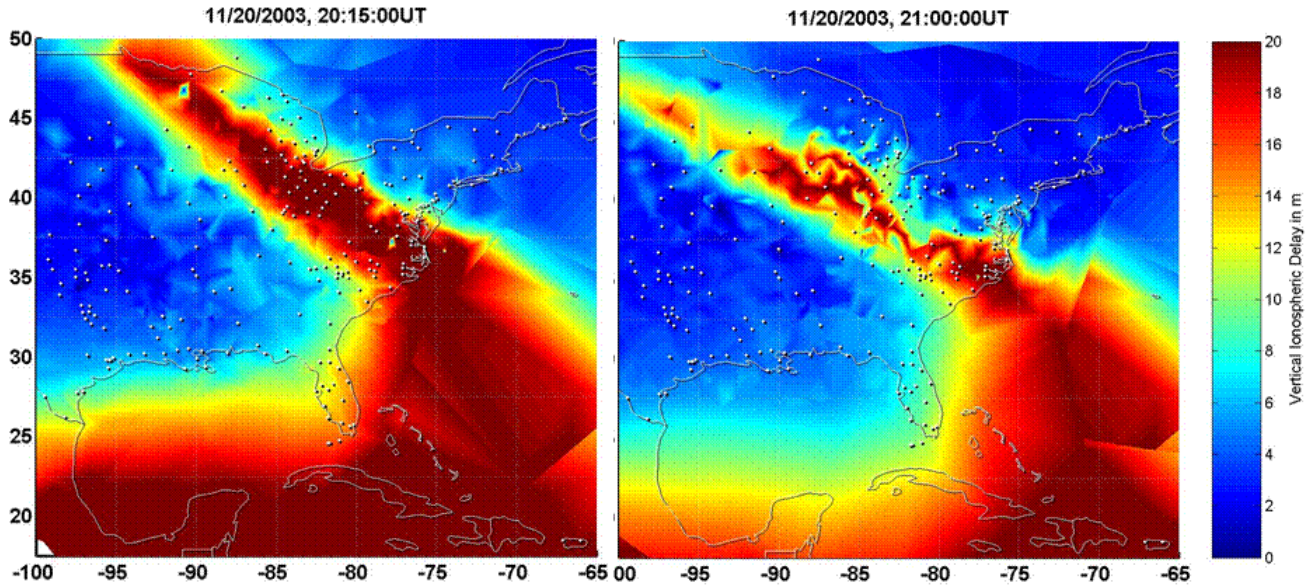

Figure 3: Extreme Ionospheric Behavior over CONUS on 20 November 2003 [15]

systems. However, it has several important weaknesses compared to average risk. The first is that the degree of risk aversion preferred by aviation is buried within the hazard probabilities generated by specific risk – it cannot be separated out. This means that specific-risk results do not translate well to other classes of users, as very few users would happen to have the same risk preferences that have evolved within aviation over several decades.

In addition, specific risk makes a distinction between unknown events that could be known and those that are both rare and completely unknowable. Unusual wind conditions, for example, might catch a single aircraft by surprise, but it they are anything but extremely small-scale, they should be observable to the airspace system as a whole and could not be considered as random. In other words, they must be treated as having a probability of 1.0 despite being very rare [3]. A very risk-averse "value of information" can be inferred from this principle, but it is much different than the "risk neutral" one built into PRA, as it severely penalizes systems that do not include all potentially-informative sensors. Since each sensor added to a system provides less benefit than the last, almost all cost-effective systems fall into this category.

2.3 Comparative Example: Severe Ionospheric Spatial Decorrelation

This section highlights the unusual features of specific risk assessment by examining how SBAS and GBAS mitigate a unique threat to augmented GNSS – the possibility of extreme ionospheric spatial decorrelation. Figure 3 (from [15]) shows the most severe event of this type observed to date in the Conterminous United States (CONUS). In it, a banded region of very high ionospheric delay (in red) is surrounded by regions of much lower delay (in blue) to the East and West. Under these very rare conditions, gradients of 400 mm/km can exist between the measurements used to generate SBAS and GBAS corrections and those applied by aircraft and other users, resulting in position errors of 5 – 10 meters or more (see [15,16] for details).

Because SBAS and GBAS users are threatened by this phenomenon in somewhat different ways, the worst-case "threat models" developed for them are very different. With a large network of widely-distributed stations, SBAS is able to observe, detect, and exclude almost all unusual ionospheric features before users are affected by the largest possible gradients [16]. The extreme event shown in Figure 3 was detected by the FAA WAAS system before it generated any significant user errors. Therefore, the "worst case" for SBAS users is not the feature that generates largest possible gradient but instead the feature that causes the maximum errors while being just small enough (in geographical size and ionospheric gradient) to escape SBAS detection and exclusion. The SBAS threat model for this theoretical worst-case event is quite detailed and intricate [17]. In contrast, an individual GBAS ground station at a particular airport has no guarantee of observing a threatening gradient before it affects approaching aircraft. In most cases, the resulting anomalous ionospheric rate of change will cause detection and exclusion before possibly hazardous errors occur, but this cannot be guaranteed, as a large spatial gradient can coexist with a minimal temporal gradient. Therefore, the GBAS threat model emphasizes the largest possible gradient and the worst possible alignment of ground system, approaching aircraft, and satellite geometry [15].

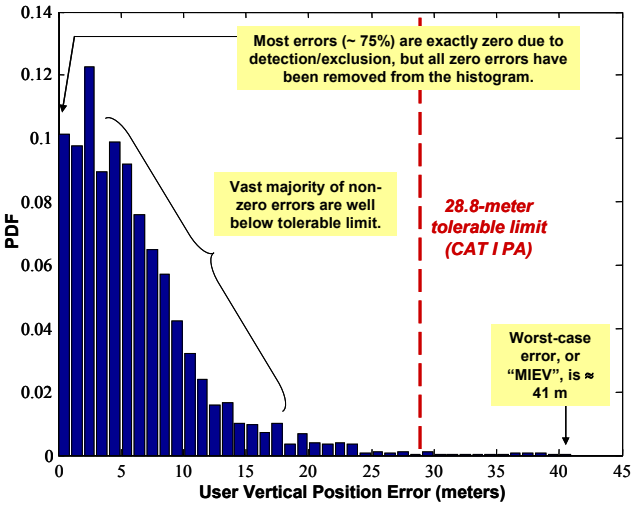

Figure 4: Ionosphere-Gradient-Induced Vertical Position Errors for LAAS System at Memphis [15]

Figure 4 (from [15]) shows the results of a simulation of "near-worst-case" ionospheric gradients for a GBAS station at Memphis supporting CAT I precision approaches. The simulation included the full range of geometric parameters in the threat model for LAAS in CONUS [15] except for the maximum gradient (425 and 375 mm/km) and all possible ground-aircraft-GPS satellite geometries and timings (using the SPS-standard 24-satellite constellation from [18]). About 75% of the trials resulted in zero user error because monitor detection and exclusion occurred before the ionospheric gradient affected the simulated aircraft, but these cases are not included in the histogram. Of the remainder, most vertical position errors are below 10 m, and almost all are below 25 m, but LAAS is forced to mitigate the worst-case error of 41 m according to the principles of specific risk. Remember that this scenario represents a rare event to begin with. While the prior probability of this event is hard establish precisely, an approximate distribution suitable for PRA was developed but could not be used [6].

This example demonstrates how the conservatism implicit in specific risk assessment penalizes users. Although PRA would show that the combination of factors needed to produce a 40-meter error is exceedingly improbable (almost certainly below 10^{-10} per approach), specific risk forces the entire GBAS mitigation effort to be targeted entirely at this scenario. In this case, since monitoring is not guaranteed to detect the anomaly in time, the only recourse is *geometry screening* – a cumbersome method in which the ground system continually evaluates the worst-case error and, if it exceeds the 28-meter tolerable limit at the CAT I decision height, determines which broadcast parameters to inflate such that all possible satellite geometries causing worst-case errors exceeding 28 meters are made unavailable (i.e., have the inflated VPL larger than the 10-meter CAT I VAL) [2,15]. The result of this procedure is much lower user availability than would be achieved without inflation [19,24]. SBAS pays a similar penalty, as we will see in Section 3.0 – the broadcast GIVE values that bound worst-case ionospheric errors (and thus the resulting protection levels) are much higher than they would be if the worst-case error were not the dominant concern.

To the extent that unneeded loss of system availability represents a safety issue at the airspace level, the worst-case focus that results from specific risk is not optimal even from a safety standpoint. But this is not the only concern. Specific risk requires a great deal of development and testing to identify and mitigate a handful of very peculiar, non-representative conditions. When schedule and resources are limited, other potential threats that are easier to foresee but seem extremely improbable are often neglected. One example is the treatment of multiple hardware failures. If individual failures are assumed to be statistically independent, the probability of multiple simultaneous failures is very small. However, while statistical independence is a common assumption in math classes because it makes calculations much easier, it rarely applies in the real world. Because satellites and ground receivers are similar, if not identical, the presence of a failure in one unit may suggest a common cause or at least a common vulnerability, meaning that the probability of additional failures is much higher than independence would suggest [4,6]. Thus, assuming independence by default could lead to neglecting entire categories of risk that are more threatening (based on PRA) than the "worst-case" events deemed credible by specific risk.

3.0 STUDY OF MAXIMUM WAAS ERRORS AND PROTECTION LEVELS

In order to investigate the conservatism built into SBAS and GBAS specific risk assessment, maximum WAAS horizontal and vertical position errors over time as measured by the Performance Analysis Network (PAN) maintained by the William J. Hughes FAA Technical Center have been examined and compared to the protection levels that applied when the maximum errors occurred. The earliest PAN reports for WAAS extend back to 2000, well before initial WAAS commissioning in July 2003. This study begins shortly after commissioning, beginning with PAN Report #8 (covering January to March 2004) and extending through the most recent PAN Report #34 (covering July to September 2010). Note that each PAN report covers three months of observed WAAS performance [20,21].

Figure 5 shows the 38 WAAS reference stations (WRSs) used by the PAN to collect position error and protection level information (some of these stations were not used in earlier PAN reports) [22]. While measurements from these stations are used to generate WAAS

Figure 5: WAAS PAN Reference Station Network [22]

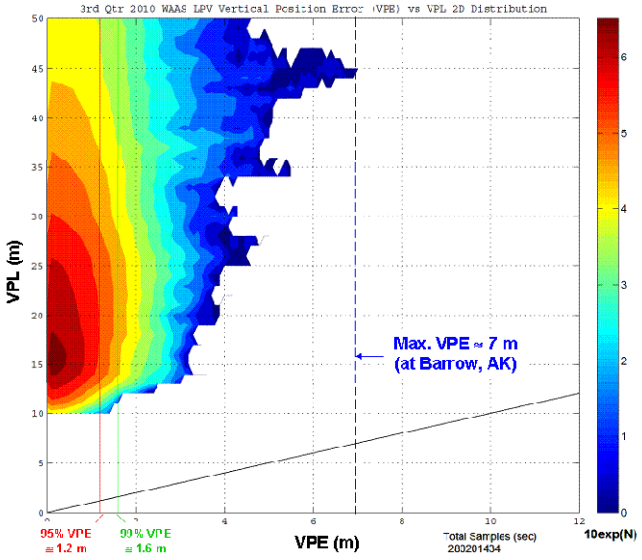

Figure 6: WAAS VPL vs VPE (June – Sept. 2010) [20]

corrections and error bounds, they are also used by the PAN as static "pseudo-users" that compute WAAS-corrected positions and protection levels according to the aircraft user algorithms specified in the WAAS MOPS [1]. The resulting positions are compared to the known, pre-surveyed positions of each station to derive estimates of vertical and horizontal position errors (VPE and HPE) once per second.

Figure 5 indicates three sets of stations are shown based on their quality of WAAS coverage. These sets are unofficial and were created only for the purposes of this study. The 7 stations in the "Inner" set are expected to have good WAAS coverage at all times because they are surrounded by other stations. The 13 stations in the "Outer" set are expected to have "acceptable" but "less good" coverage because some of them are at the edges of CONUS and have limited coverage from the set of 18 "Remote" stations. The "Remote" stations themselves are there to provide coverage to the "Inner" and "Outer" regions as well as to provide the best possible coverage of Alaska, southern Canada, northern Mexico, and the Gulf of Mexico and Caribbean. Because the "Remote" stations extend beyond the primary coverage region of WAAS in CONUS, errors at these stations are not considered in this section. However, the tables in the Appendix show the results for the Remote station set as well as for the Inner and Outer stations.

Figure 6 is a 2-D plot of position error vs. protection level in the vertical axis (i.e., VPE vs. VPL) for all epochs and stations during the three months (July 1 – September 30, 2010) covered by the most recent WAAS PAN Report #34 [20]. As will be demonstrated shortly, these results are typical of the entire period since WAAS commissioning in 2003, particularly the last several years. The vertical lines on the plot indicate the 95th-percentile, 99th percentile, and maximum VPEs in this period (1.2 m, 1.8 m, and 7 m). The maximum VPE occurred at Barrow, AK, which is one of the most remote stations in the WAAS network (see Figure 5). In comparison, the very lowest VPLs (intended to be 1 – 10^{-7} bounds on VPE) are in the range of 10 – 15 m, and values as high as 40 meters are not uncommon. The most demanding approach operation that WAAS supports, LPV, allows approaches to a 200 ft minimum decision height (DH) and requires that VPL be below a VAL of 35 meters (HPL must also be below a HAL of 45 meters) [1]. When this is not the case, the approach operation is not available; thus these higher VPLs extract a significant cost.

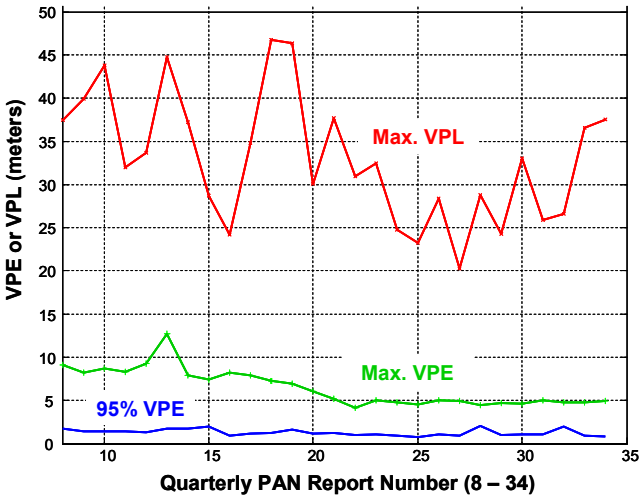

Figure 7: WAAS *Vertical* Errors and Protection Levels from 2004 – 2010

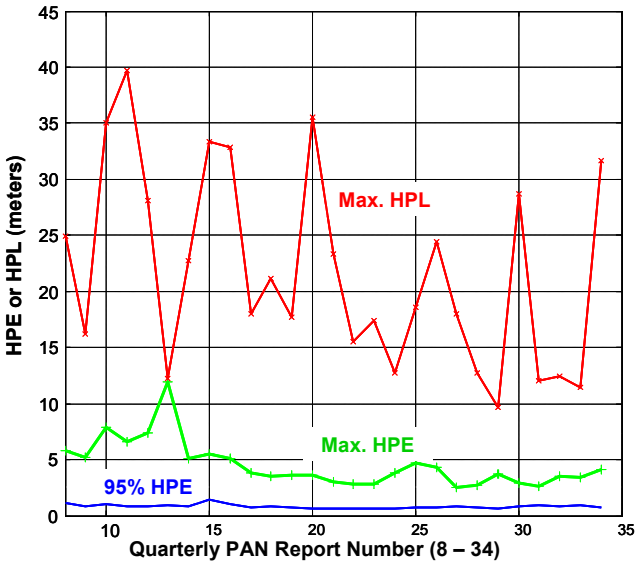

Figure 8: WAAS *Horizontal* Errors and Protection Levels from 2004 – 2010

Figures 7 (for vertical errors) and 8 (for horizontal errors) span the entire period of WAAS PAN Reports used in this study. The data plotted in these figures is shown in detail in Tables A1 (vertical) and A2 (horizontal) in the Appendix, where it is broken out by "Inner," "Outer," and "Remote" station sets. As explained above, errors at Remote stations are not shown in these plots because they are not fully representative of WAAS performance. In addition, because the maximum Inner and Outer station errors are similar, these plots show results for the maximum "Inner/Outer" set. Specifically, the "Max. VPE" shown in Figure 7 corresponds to the VPE at the station with the largest VPE across all stations in the Inner and Outer station sets in each quarterly PAN report. The "95% VPE" corresponds to the 95th-percentile VPE at that station (not over all stations, as in Figure 6). The "Max.

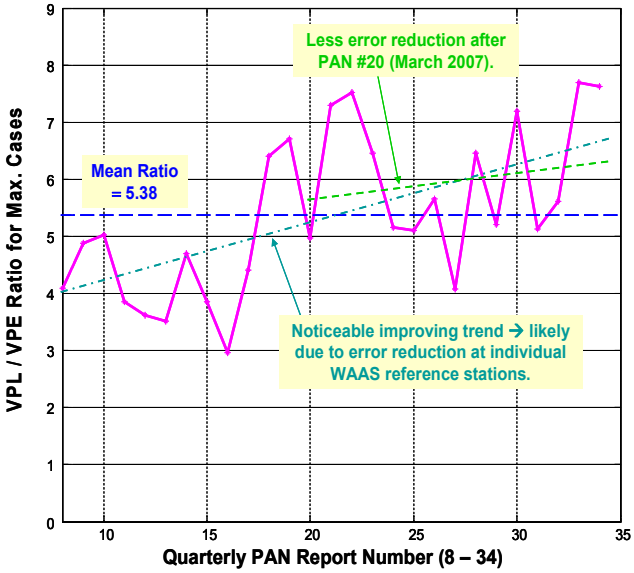

Figure 9: Ratio of VPL to VPE from 2004 – 2010

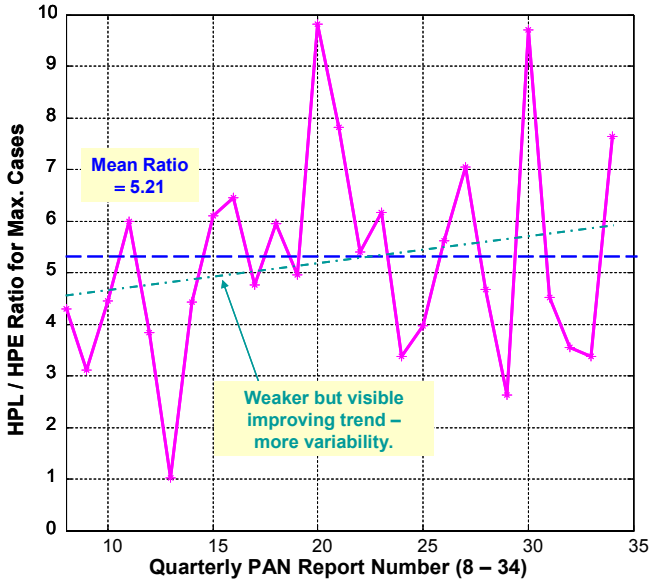

Figure 10: Ratio of HPL to HPE from 2004 – 2010

VPL" represents the VPL *at the station and time of the maximum VPE* – it is not the "largest VPL" recorded at a particular station. The horizontal errors shown in Figure 8 are defined analogously, and note that the station that observes the largest horizontal error in a given quarterly PAN report may differ from the one that observes the largest vertical error.

Figures 7 and 8 demonstrate that, while both 95% and maximum errors are quite low and are within the expected range of each other, the WAAS protection levels associated with the maximum errors greatly exceed them. This pattern is clearer in Figure 7 for vertical errors because maximum VPL tends to be more consistent across PAN reports, but it is true for horizontal errors as

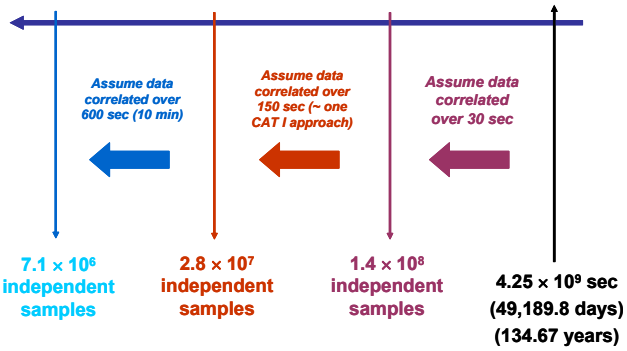

Figure 11: No. of Independent Samples in PAN Data

well. Figures 9 and 10 clarify this relationship by plotting the ratio of VPL to VPE and HPL to HPE for the station and time of the maximum error. The mean of this ratio is very high and is about the same in both cases: 5.38 for vertical and 5.21 for horizontal. Figure 9 shows a steady upward trend in the ratio that is mostly due to WRS improvements that resulted in maximum VPE being reduced over time. This trend is clearly visible in Figure 7 and appears to exceed the weaker trend of lowering VPL due to WAAS algorithm enhancements. The same trend is visible in the horizontal Figures 8 and 10 but is weaker due to the greater variability of HPL over time.

A couple of specific cases of very large errors should be mentioned. One of these is visible in Figures 8 and 10 and is due to a reported maximum HPE of 11.962 m at the Cleveland WRS in PAN Report #13 (see Table A2 in the Appendix) [21]. The reported HPL, 12.194 m, just exceeded this error, resulting in a ratio very close to 1.0 in Figure 10. This event stands out in Figures 8 and 10 because the nearly-12-meter HPE is far greater than any other recorded in the PAN reports and because the ratio in Figure 10 drops to near 1.0. However, other information in PAN Report #13 makes this error suspect and suggests that no unusual error occurred. In particular, Table 5-1 of this report gives "safety margin indices" which are similar to the ratios shown in Figures 9 and 10. The horizontal index shown for Cleveland in this table is 4.29 instead of a number near 1.0, suggesting a much lower maximum HPE of around 3 meters, which is typical for the Cleveland WRS. Another source of very large errors (as high as 37.5 meters) at remote stations in Alaska is ionospheric scintillation in the auroral region. WAAS Discrepancy Report (DR) #52 shows examples of the resulting large range and position domain errors at Fairbanks and other Alaskan reference stations [23]. While ionospheric scintillation can cause significant errors, errors above 10 meters would be very surprising. After investigation, it became evident that the original reference receivers were flawed in that they did not lose lock and stop tracking the affected satellites but instead continued to extrapolate and report highly erroneous measurements. These receivers were replaced, and very large errors due to scintillation have disappeared.

To evaluate the significance of the large PL-to-max-PE ratios in the WAAS PAN database, we need to approximate the number of independent samples from which the maximum errors were derived. As noted before, WAAS protection levels represent error bounds at the $1 - 10^{-7}$ probability level based on specific risk. With one measurement being collected at each operational station every second, a total of about 4.25 billion samples were collected in the PAN reports from January 2004 to September 2010. Note that measurements from "Remote" stations are included in this count, but they are also represented in the conclusions because their PL-to-max-PE ratios are very similar to the ones shown in Figures 9 and 10. Figure 11 shows how the total number of samples would be adjusted based on different assumptions of how many seconds separates statistically independent samples. This interval is hard to determine because the time correlation of rare-event errors depends upon many potential factors, not all of which are understood or even identified. The authors' best guess of an approximation to this interval is between 30 and 150 seconds, meaning that the PAN database contains between 2.8×10^7 and 1.4×10^8 independent samples. Since the WAAS protection levels are consistently much larger than the maximum position errors, it is likely that they are very conservative from the perspective of average risk.

4.0 PROTECTION-LEVEL ADJUSTMENT FOR "AVERAGE RISK" USERS

4.1 Protection Level Reduction for WAAS Users

Using the results in Section 3, a preliminary estimate of the reduced WAAS protection levels that would apply to "average risk" users can be made. Figure 12 shows a comparison between the actual 95% WAAS VPL and HPL and the "adjusted" VPL and HPL might be achievable with WAAS (for the same $1 - 10^{-7}$ bounding probability) for "average risk" users. The actual WAAS VPLs are taken from the more recent WAAS PAN Reports starting from #24 (covering January to March 2008) as the period from 2008 to the present includes most of the WAAS algorithm improvements introduced since commissioning in 2003. The actual 95% VPLs and HPLs represent the largest reported 95th-percentile values among the stations in CONUS for each quarterly period (note that the stations in CONUS match the combined "Inner/Outer" set from Figure 5 except for the Winnipeg WRS). The lower adjusted VPLs and HPLs are derived by dividing each VPL by a factor of 4.0 and each HPL by a factor of 2.5. These two reduction factors are derived from Figures 9 and 10, respectively, as conservative estimates of the ratio between protection levels and maximum position errors. Note that the factor of 2.5 for horizontal errors does not include the 12-meter error in Cleveland from PAN Report #13 discussed above, as this is thought to be spurious or non-representative.

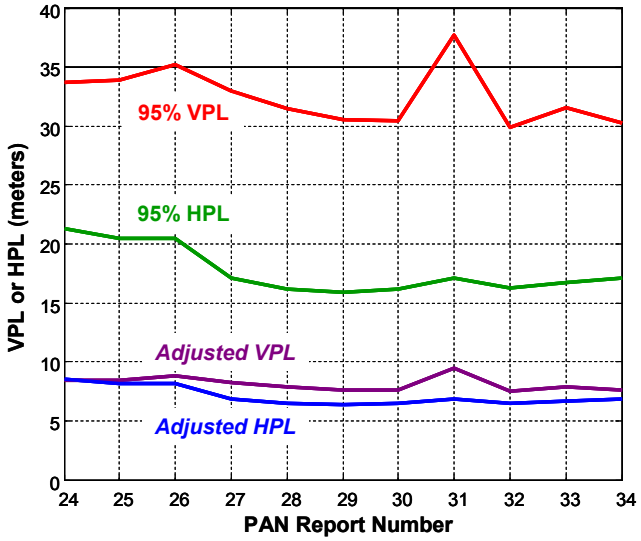

Figure 12: Projected WAAS Protection Level Reductions for "Average Risk" Users

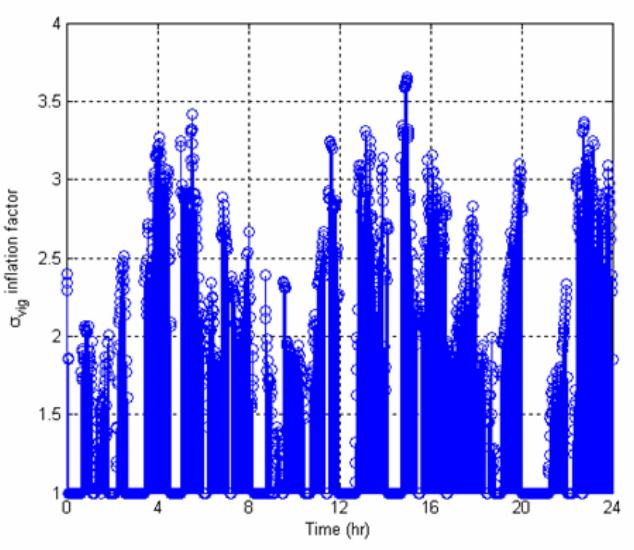

Figure 13: Typical σ_{vig} Inflation Factors for CAT I LAAS [24]

While projections based on these reduction factors are imprecise, they demonstrate the much lower error bounds that non-aviation users with an average risk safety perspective could achieve. Most non-aviation users will be primarily concerned with horizontal error bounds. Figure 12 suggests that the typical 95% WAAS HPLs of 15 – 20 meters (for the worst location in CONUS) can be reduced to 6 – 8 meters and still provide a confident $1 - 10^{-7}$ error bound. This difference would be significant for many classes of ground and marine transportation users. For some users, the reduction would allow operations with tighter physical safety margins to be supported. For others, the benefit would be much higher availability, as a 25-meter HAL could be supported by much poorer satellite geometries than would otherwise be the case.

It is important to emphasize that these preliminary projections for "average risk" users are just that. In order to formally establish new integrity requirements and protection levels for existing systems, the "Hazardously Misleading Information" or "HMI" analyses previously done for these systems need to be redone using the principles of PRA and average risk [3]. While the original development of the WAAS and LAAS HMI analyses was lengthy and resource-intensive, almost all of the detailed work is already complete. As long as the original analyses are available, it is a much smaller task to take these raw results and create PRAs out of them by extracting the original specific-risk assumptions and applying average-risk principles instead.

4.2 Protection Level Reduction for LAAS Users

Since the first GBAS ground station design (the Honeywell SLS-4000 LAAS Ground Facility) was certified for CAT I use in 2009 and has not yet been approved for operations at a specific airport, much less data is available to do a preliminary analysis for GBAS similar to the one done for WAAS above. However, the degree of sigma inflation in the parameters broadcast by CAT I LAAS is approximately known, meaning that it can be more-precisely removed from the current LAAS protection levels to estimate what they would be for average-risk users. Figure 13 shows the degree of inflation applied to the broadcast $\sigma_{vertical\_iono\_gradient}$ (or σ_{vig}) parameter in order to protect against the worst-case ionospheric anomaly described in Section 2.3. This result is for the SPS-standard 24-satellite constellation [18] over a 24-hour period at the LAAS installation at Newark Airport (EWR), NJ using a method similar but not identical to the algorithm used in the Honeywell SLS-4000 [24]. While not all epochs require inflation, a majority t cause the nominal σ_{vig} value to be increased by a factor of 2 or more, which significantly decreases CAT I availability and currently makes it impossible to use LAAS for non-CAT-I operations using the Differentially Corrected Positioning Service (DCPS) [14].

Because of the extreme rarity of the worst-case event that dictates this inflation, it would likely not be needed for "average risk" users. Figure 14 shows how much the σ_{vig} inflation in Figure 13 increases the LAAS VPL at Newark for the standard 24-satellite constellation. The VPL reduction from removing the inflation is not as dramatic as the potential reductions shown for WAAS in Figure 12, but they are significant relative to the 10-meter VAL for LAAS CAT I approaches. Furthermore, the pre-inflated "nominal" value of σ_{vig} for LAAS is 6.4 mm/km, which is much higher than the actual one-sigma nominal gradient value of 1 – 2 mm/km because, under specific risk, the very worst nominal data must be bounded and because

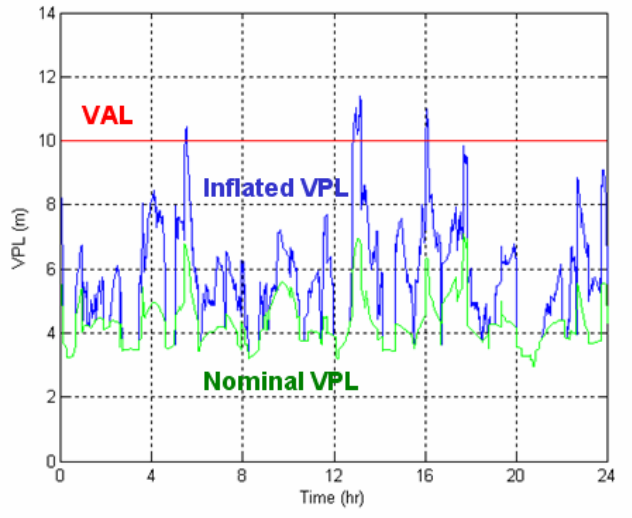

Figure 14: Impact of σ_{vig} Inflation on LAAS VPL [24]

worst-case tropospheric gradients are also bounded by σ_{vig} [25,26]. Other broadcast parameters that affect VPL, such as σ_{pr_gnd} and the ephemeris P-value that bounds worst-case ephemeris failures [2], would also be reduced significantly by switching to average risk. Overall, it is likely that LAAS protection levels based on average risk would be reduced from the current specific-risk PLs by about the same range of factors (2 – 5) as observed from WAAS data in Section 4.1.

5.0 MIXTURE OF AVERAGE AND SPECIFIC RISK REQUIREMENTS

The discussion in this paper assumes that most non-aviation users that are not encumbered by the history of aviation safety standards development will prefer to quantify risk using PRA and the "average risk" approach. This is because, as explained in Section 2.1, average risk has the enormous advantage of separating risk quantification from risk aversion. This suggests that, regardless of how risk-averse or "conservative" a given operator or decision maker is, his or her model of risk aversion can be applied most efficiently to a "risk neutral" calculation of risk that fairly represents all aspects of uncertainty. Inserting risk aversion into the calculation of risk, as done in the "specific risk" approach, is both inefficient and non-optimal from a safety perspective because extensive focus on a few extreme worst-case events drives attention away from other, less threatening but more probable events.

Having said that, it is possible that government providers of non-aviation train and marine services will want to borrow from the experience of aviation and use elements of specific risk in their safety requirements. If so, it should be noted that specific-risk requirements can be added to or "mixed with" an average-risk safety approach.

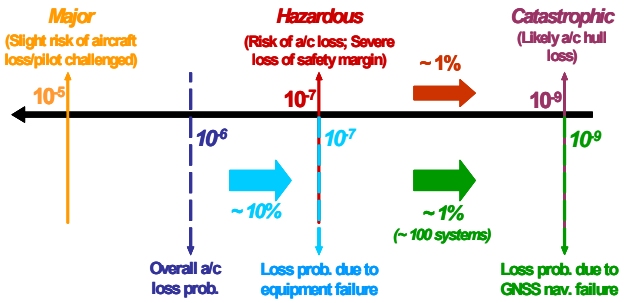

Figure 15: Simplified Total Aircraft Risk Model

One way to illustrate this is to utilize the simplified model of total aircraft accident risk derived from the *FAA System Safety Handbook* [27] and a 1994 paper on Required Navigation Performance (RNP) for GNSS [28]. In this model, which is illustrated in Figure 15, the total risk of aircraft loss per flight is roughly 10^{-6}. Equipment failure accounts for 10% of this risk, and assuming roughly 100 different systems on the aircraft, each system is allocated 10^{-9} per flight. Therefore, a system failure that likely leads to aircraft loss, such as misleading information during a CAT III approach down to the runway, is treated as "catastrophic" and must be mitigated to a probability of 10^{-9}. Similarly, a failure that might lead to aircraft loss, such as misleading information during a CAT I approach down to 200 ft, is treated as "hazardous" and must be mitigated to 10^{-7}. This difference between "catastrophic" and "hazardous" implies that hazardous events have a probability of roughly 0.01 of leading to aircraft loss. "Specific risk" is introduced by the fact that each threatening event is analyzed separately instead of being probabilistically combined. Therefore, *each* event that could lead to a "hazardous" condition must be mitigated to $1 - 10^{-7}$. Worst-case events that cannot be shown to be less probable than 10^{-7} tend to dominate all other apparently "lesser" threats.

Since this risk-allocation approach is compatible with average risk, the same probability requirements for "catastrophic" and "hazardous" events can be assigned but for "average risk" definition. In this case, the risk aversion is present in the required probabilities for "catastrophic" and "hazardous" events and how they trace back to the overall risk of aircraft loss, which should always be the focus of PRA. Adding more risk aversion could be as simple as reducing the tolerable aircraft loss risk from 10^{-6} to 10^{-7} per flight and "flowing down" this reduced allocation to make the requirements for "catastrophic" and "hazardous" events tighter accordingly (to 10^{-10} and 10^{-8}, respectively).

If we now switch to the "specific risk" perspective, what a risk-averse decision maker might want to add is the requirement that the risk of a worst-case SBAS or GBAS failure would not "materially" increase the total aircraft loss risk. For example, starting from the existing aircraft

loss risk of 10^{-6} per flight, the risk of a worst-case failure does not increase the total risk by more than a factor of 2 (i.e., to 2 × 10-6 per flight). This appears to be a conservative requirement, but it is less conservative than today's specific-risk interpretation, which requires the worst-case impact of all equipment failures to fit within the nominal 10^{-6} risk budget. If 2×10^{-6} were the maximum allowed aircraft risk from the worst-case "hazardous" GNSS failure, an additional aircraft risk allocation of 10^{-6} per approach (i.e., over and above the nominal 10^{-6} risk) would be available solely to worst-case GNSS failures. In other words, two GNSS integrity-risk requirements would apply simultaneously: 10^{-7} under the "average risk" interpretation and 10^{-6} under the "specific risk" interpretation.

In this example, it is likely that the specific-risk requirement would still dominate, but that would change as the decision maker grows more tolerant of increased total system risk from worst-case equipment failures. The point is that GNSS system developers who utilize PRA as their primary risk tool retain the flexibility to simultaneously define specific-risk-like "worst-case" integrity requirements that must also be met. Very little is given up by the use of PRA and average risk as the primary basis for GNSS user integrity risk assessment.

6.0 SUMMARY

This paper explains the differences between the "average risk" interpretation of safety used in most fields and the "specific risk" approach that has developed from civil aviation safety assessment and is now built into SBAS and GBAS integrity algorithms. SBAS and GBAS broadcasts are freely available to all GNSS users, most of whom will have different definitions of acceptable risk. These users are not optimally served at present and may hesitate to take advantage of SBAS and GBAS as a result.

Using years of collected data for the FAA WAAS system and analysis of the inflation factors built into the CAT I version of the FAA LAAS system, it appears that "average risk" users of WAAS and LAAS would be adequately supported by protection levels that are 2 to 5 times lower than those currently derived by aviation users. While these estimates have not yet been validated by full-scale probabilistic risk assessments, it is clear that the existing protection levels are much too high to represent "average risk" users, and the fact that different approaches used to examine WAAS and LAAS suggest similar levels of over-conservatism lends credence to these estimates. Therefore, we conclude that non-aviation users willing to accept "average risk" would obtain much better performance and availability from simple modifications to the existing SBAS and GBAS protection level calculations specified for aviation users.

ACKNOWLEDGMENTS

The authors would like to thank the FAA Satellite Navigation Program Office for its support of their research on WAAS and LAAS. However, the opinions expressed here are solely those of the authors. The authors would like to thank Jim Kelly and Tim Murphy for their explanations of the evolution of today's SBAS and GBAS integrity requirements. They would also like to thank the FAA Technical Center for its efforts in collecting and publishing WAAS error data over the last decade using its Performance Analysis Network (PAN).

REFERENCES

[1] *Minimum Operational Performance Standards for Global Positioning System/Wide Area Augmentation System Airborne Equipment*. Washington, DC, RTCA SC-159, WG-2, DO-229D, Dec. 13, 2006. http://www.rtca.org

[2] *Minimum Operational Performance Standards for GPS Local Area Augmentation System Airborne Equipment*. Washington, DC, RTCA SC-159, WG-4, DO-253C, Dec. 16, 2008. http://www.rtca.org

[3] T. Walter, P. Enge, B. DeCleene, "Integrity Lessons from the WAAS Integrity Performance Panel (WIPP)," *Proc. ION NTM 2003*, Anaheim, CA, Jan. 22-24, 2003, pp. 183-194. http://waas.stanford.edu/~wwu/papers/gps/PDF/WalterIONNTM03.pdf

[4] S. Pullen, "Providing Integrity for Satellite Navigation: Lessons Learned (Thus Far) from the Financial Collapse of 2008-2009," *Proc. ION GNSS 2009*, Savannah, GA, Sept. 22-25, 2009, pp. 1305-1316. http://waas.stanford.edu/~wwu/papers/gps/PDF/PullenIONGNSS09.pdf

[5] S. Pullen, "System Overview, Recent Developments, and Future Outlook for WAAS and LAAS," *Proc. Tokyo Univ. Mercantile Marine GPS Symp.*, Tokyo, Japan, Nov. 11-13, 2002. http://waas.stanford.edu/~wwu/papers/gps/PDF/PullenTokyo02.pdf

[6] S. Pullen, J. Rife, P. Enge, "Prior Probability Model Development to Support System Safety Verification in the Presence of Anomalies," *Proc. IEEE/ ION PLANS 2006*, San Diego, CA, April 24-27, 2006, pp. 1127-1136. http://waas.stanford.edu/~wwu/papers/gps/PDF/PullenIONPLANS06.pdf

[7] M. Stamatelatos, *et al*, "Probabilistic Risk Assessment Procedures Guide for NASA Managers and Practitioners," Office of Safety and Mission Assurance, NASA Headquarters, Washington, DC, Version 1.1, Aug. 2002. http://www.hq.nasa.gov/office/codeq/doctree/praguide.pdf

[8] "Risk Aversion," in *Wikipedia*. Retrieved Feb. 7, 2011. http://en.wikipedia.org/wiki/Risk_aversion

[9] "Value of Information," in *Wikipedia*. Retrieved Feb. 7, 2011. http://en.wikipedia.org/wiki/Value_of_information

[10] S. Pullen, "A Comparative Overview of the Protection Level Concept for Augmented GNSS and LORAN," Stanford University, GPS Laboratory Meeting, Dec. 20, 2002. http://www.stanford.edu/~spullen/GNSS_PL_concept_2002.ppt

[11] *Minimum Aviation System Performance Standards for the Local Area Augmentation System (LAAS)*. Washington, D.C., RTCA SC-159, WG-4, DO-245A, Dec. 9, 2004. http://www.rtca.org

[12] J. Rife, R.E. Phelts, "Formulation of a Time-Varying Maximum Allowable Error for Ground-Based Augmentation Systems," *Proc. ION NTM 2006*, Monterey, CA, Jan. 18-20, 2006, pp. 446-453. http://waas.stanford.edu/~wwu/papers/gps/PDF/RifeIONNTM06.pdf

[13] *Criteria for Approval of Category III Weather Minima for Takeoff, Landing, and Rollout*. US Dept. of Transportation/Federal Aviation Administration, Washington, DC, AC 120-28D, July 13, 1999. http://preview.tinyurl.com/AC120-28D http://preview.tinyurl.com/AC120-28D-appx

[14] T. Murphy, M. Harris, Y.S. Park, S. Pullen, "GBAS Differentially Corrected Positioning Service Ionospheric Anomaly Errors Evaluated in an Operational Context," *Proc. ION ITM 2010*, San Diego, CA, Jan. 25-27, 2010, pp. 394-410. http://waas.stanford.edu/~wwu/papers/gps/PDF/MurphyIONITM10.pdf

[15] S. Pullen, Y.S. Park, P. Enge, "Impact and Mitigation of Ionospheric Anomalies on Ground-Based Augmentation of GNSS," *Radio Science*, Vol. 44, Aug. 8, 2009. http://www.agu.org/journals/rs/rs0904/2008RS004084/

[16] S. Datta-Barua, "Ionospheric Threats to Space-Based Augmentation System Development," *Proc. ION GNSS 2004*, Long Beach, CA, Sept. 21-24, 2004, pp. 1308-1317. http://waas.stanford.edu/~wwu/papers/gps/PDF/DattaBaruaIONGNSS04.pdf

[17] J. Blanch, T. Walter, P. Enge, "Ionospheric Threat Model Methodology for WAAS," *Proc. ION 2001 Annual Meeting*, Albuquerque, NM, June 11-13, 2001, pp. 508-513. http://waas.stanford.edu/~wwu/papers/gps/PDF/juanionam01.pdf

[18] *Global Positioning System Standard Positioning Service Performance Standard*. U.S. Department of Defense, Washington, DC, 4th Edition, Sept. 2008. http://www.pnt.gov/public/docs/2008/spsps2008.pdf

[19] S. Ramakrishnan, J. Lee, *et al*, "Targeted Ephemeris Decorrelation Parameter Inflation for Improved LAAS Availability during Severe Ionosphere Anomalies," *Proceedings of ION 2008 National Technical Meeting*, San Diego, CA., Jan. 28-30, 2008, pp. 354-366. http://waas.stanford.edu/~wwu/papers/gps/PDF/RamakrishnanIONNTM08.pdf

[20] "Wide-Area Augmentation System Performance Analysis Report," Report #34, Reporting Period: July 1 – Sept. 30, 2010, FAA/William J. Hughes Technical Center, Atlantic City, NJ, Oct. 2010. http://www.nstb.tc.faa.gov/REPORTS/waaspan34.pdf

[21] "Wide-Area Augmentation System Performance Analysis Report," Reports #8-33, Covering Reporting Periods: Jan. 1, 2004 – June 30, 2010, FAA/William J. Hughes Technical Center, Atlantic City, NJ. http://www.nstb.tc.faa.gov/DisplayArchive.htm

[22] *GNSS – Satellite Navigation* (Press Kit), U.S. Dept. of Transportation, Federal Aviation Administration, Washington, DC, Nov. 2008. http://preview.tinyurl.com/4ofdzz4

[23] N. Rosen, D. Nelthropp, B. McDonnell, "DR#52: Ionospheric Scintillation caused High Position Errors at Fairbanks," WAAS Technical Report, William J. Hughes Technical Center, Pomona, NJ, May 2, 2007. http://preview.tinyurl.com/WAAS-DR52

[24] J. Lee, J. Seo, Y.S. Park, S. Pullen, P. Enge, "Ionospheric Threat Mitigation by Geometry Screening in GNSS Ground Based Augmentation Systems," Submitted to *AIAA J. of Aircraft*, Oct. 2010 (forthcoming). http://www.aiaa.org

[25] J. Lee, S. Pullen, S. Datta-Barua, P. Enge, "Assessment of Ionosphere Spatial Decorrelation for Global Positioning System-Based Aircraft Landing Systems," *AIAA. J. of Aircraft*, Vol. 44, No. 5, Sept.-Oct. 2007, pp. 1662-1669. http://preview.tinyurl.com/JA-N5-07

[26] Z. Zhu, F. van Graas, "Tropospheric Delay Threats for the Ground Based Augmentation System," *Proc. ION ITM 2011*, San Diego, CA, Jan. 24-26, 2011 (forthcoming). http://www.ion.org

[27] *FAA System Safety Handbook*, U.S. Dept. of Transportation, Federal Aviation Administration, Washington, DC, Updated May 21, 2008. http://www.faa.gov/library/manuals/aviation/risk_management/ss_handbook/

[28] R. Kelly, J. Davis, "Required Navigation Performance (RNP) for Precision Approach and Landing with GNSS Application," *Navigation*, Vol. 41, No. 1, Spring 1994, pp. 1-30. http://ion.org/search/view_abstract.cfm?jp=j&idno=106

APPENDIX: WAAS ERROR DATA TABLES FROM PAN REPORTS

PAN Report	Inner WRS	Inner VPE_95%	Inner VPE_Max	Inner VPL	Outer WRS	Outer VPE_95%	Outer VPE_Max	Outer VPL	Remote WRS	Remote VPE_95%	Remote VPE_Max	Remote VPL	No. PA Sites	Ave. No. Days
8	Chicago	1.086	7.541	49.612	Minneapolis	1.710	9.133	37.430	N/A	N/A	N/A	N/A	20	88.85
9	Dallas	1.442	8.191	39.956	Minneapolis	1.695	7.794	40.806	N/A	N/A	N/A	N/A	20	90.80
10	Dallas	1.388	8.722	43.829	Minneapolis	1.790	7.376	32.210	N/A	N/A	N/A	N/A	20	92.00
11	Dallas	1.371	8.280	31.969	Minneapolis	1.501	8.034	37.367	N/A	N/A	N/A	N/A	20	90.55
12	Dallas	1.298	9.301	33.699	Salt Lake City	1.155	8.581	47.939	N/A	N/A	N/A	N/A	20	86.90
13	Dallas	1.504	9.457	28.399	Minneapolis	1.765	12.756	44.758	N/A	N/A	N/A	N/A	20	91.00
14	Dallas (3)	1.141	6.426	26.887	Oakland	1.706	7.931	37.235	N/A	N/A	N/A	N/A	20	90.05
15	Dallas	1.469	6.719	24.612	Minneapolis	1.956	7.439	28.722	N/A	N/A	N/A	N/A	20	91.80
16	Albuquerque	0.934	8.195	24.246	Minneapolis	1.157	8.002	31.380	N/A	N/A	N/A	N/A	20	91.80
17	Dallas	1.202	7.893	34.771	Oakland	1.273	6.385	47.296	N/A	N/A	N/A	N/A	20	90.55
18	Dallas	1.210	6.888	37.435	Oakland	1.228	7.296	46.769	N/A	N/A	N/A	N/A	20	87.95
19	Dallas	1.281	6.879	35.097	Miami	1.657	6.913	46.396	Fairbanks	1.080	7.395	40.632	27	89.44
20	Dallas	1.184	6.040	30.050	Seattle	0.886	5.858	22.705	Fairbanks (1)	1.062	22.492	33.620	27	88.07
21	Dallas	1.028	5.064	26.238	Miami	1.231	5.160	37.664	Kotzebue (1)	1.183	37.308	39.902	27	89.74
22	Denver	1.281	3.975	34.868	Oakland	1.043	4.119	30.970	Fairbanks	1.118	9.255	34.793	27	90.52
23	Kansas City	0.945	5.016	24.232	Minneapolis	1.067	5.029	32.445	Puerto Vallarta	1.466	5.854	40.937	36	89.22
24	Memphis	0.889	4.800	24.742	Seattle	0.801	4.273	20.643	Tapachula	1.917	7.347	44.259	36	90.56
25	Denver	0.800	3.401	27.877	Seattle	0.766	4.553	23.230	San Juan	1.300	5.859	31.842	37	90.54
26	Denver	1.100	5.025	28.390	Oakland	1.061	4.808	23.802	S.J. Del Cabo	1.138	5.566	31.806	37	90.57
27	Denver	1.022	4.571	25.254	Seattle	0.915	4.972	20.294	Iqaluit	2.087	6.977	28.362	37	90.76
28	Chicago	0.852	4.046	21.989	Miami	2.041	4.462	28.787	Fairbanks	0.997	8.018	35.478	37	88.59
29	Cleveland	1.041	4.664	24.292	Miami	1.537	4.384	29.033	Barrow	1.128	6.733	26.198	37	90.70
30	Dallas	1.001	4.459	50.101	Wash DC	1.124	4.589	33.014	Iqaluit	1.731	9.768	42.103	36	91.50
31	Denver	1.108	5.045	25.872	Miami	1.612	4.240	24.229	Iqaluit	1.766	7.556	27.882	37	90.24
32	Cleveland	1.001	4.143	28.377	Miami	2.005	4.738	26.618	Iqaluit	1.869	8.106	45.033	37	89.43
33	Denver	0.938	4.754	36.569	Miami	1.298	4.516	30.514	Barrow	1.245	7.700	38.500	36	90.17
34	Memphis	1.048	4.070	13.567	Seattle	0.849	4.920	37.557	Barrow (2)	1.165	6.975	44.427	36	92.00
Ave		**1.132**	**6.058**	**30.849**		**1.364**	**6.232**	**33.326**		**1.391**	**10.182**	**36.611**		**90.16**
Max		**1.504**	**9.457**	**50.101**		**2.041**	**12.756**	**47.939**		**2.087**	**37.308**	**45.033**		

Notes:

(1) Very large Alaskan errors attributed to brief periods of Ionospheric Scintillation on 30 March 2007 and May 2007 in WAAS DR 52. Maximum VPE at Fairbanks (2nd Worst site in PAN 21) was 13.298 m during PAN 21 period; VPL ratio = 0.556; VPE_95% = 1.000 m.

(2) PA site count and no. days for PAN report #34 excludes Tapachula station, which was listed in Table 1-1 but showed zero days of data collection.

(3) No 95% VPE listed for Dallas in Table 2-2 of PAN #14. As a filler, 95% VPE of station with 2nd largest max. VPE among inner WRSs (Chicago) is listed instead.

Table A1: *Vertical* Error and Protection Level (in meters) from WAAS PAN Reports (Jan. 2004 – Sept. 2010)

PAN Report	Inner WRS	Inner HPE_95%	Inner HPE_Max	Inner HPL	Outer WRS	Outer HPE_95%	Outer HPE_Max	Outer HPL	Remote WRS	Remote HPE_95%	Remote HPE_Max	Remote HPL	No. PA Sites	Ave. No. Days
8	Cleveland	0.832	4.984	25.559	Minneapolis	1.184	5.798	24.884	N/A	N/A	N/A	N/A	20	88.85
9	Dallas	0.871	5.233	16.252	Oakland	0.921	4.579	36.055	N/A	N/A	N/A	N/A	20	90.80
10	Kansas City	0.636	4.951	29.647	Minneapolis	1.062	7.887	35.053	N/A	N/A	N/A	N/A	20	92.00
11	Kansas City	0.716	4.430	30.979	Houston	0.887	6.624	39.665	N/A	N/A	N/A	N/A	20	90.55
12	Cleveland	0.740	4.900	22.685	Boston	0.816	7.337	28.111	N/A	N/A	N/A	N/A	20	86.90
13	Cleveland (4)	0.923	11.962	12.194	Billings	0.765	5.262	37.856	N/A	N/A	N/A	N/A	20	91.00
14	Dallas (3)	0.696	4.842	34.340	Billings	0.854	5.133	22.712	N/A	N/A	N/A	N/A	20	90.05
15	Dallas	1.452	5.471	33.360	Oakland	1.206	5.235	38.212	N/A	N/A	N/A	N/A	20	91.80
16	Dallas	1.078	5.090	32.839	Minneapolis	1.067	3.797	18.704	N/A	N/A	N/A	N/A	20	91.80
17	Dallas	0.743	3.748	21.295	Boston	0.711	3.775	17.976	N/A	N/A	N/A	N/A	20	90.55
18	Dallas	0.825	3.072	21.483	Boston	0.807	3.553	21.149	N/A	N/A	N/A	N/A	20	87.95
19	Cleveland	0.788	3.569	17.668	Miami	1.054	3.036	33.000	Barrow (1)	0.748	8.852	25.584	27	89.44
20	Dallas	0.792	3.364	23.361	Billings	0.691	3.628	35.569	Barrow (1)	0.666	11.175	24.944	27	88.07
21	Cleveland	0.697	2.781	15.801	Minneapolis	0.640	2.988	23.344	Fairbanks (1)	0.578	9.742	18.990	27	89.74
22	Denver	0.601	2.257	22.347	Minneapolis	0.616	2.868	15.503	Barrow (1)	0.644	37.487	37.942	27	90.52
23	Albuquerque	0.615	2.817	17.389	Boston	0.715	2.507	15.475	Iqualit	0.868	5.084	30.443	36	89.22
24	Denver	0.665	2.567	23.550	Minneapolis	0.689	3.768	12.730	S.J. del Cabo	0.910	4.765	32.637	36	90.56
25	Dallas	0.606	2.835	33.353	Seattle	0.751	4.679	18.567	Iqualit	0.542	4.726	33.049	37	90.54
26	Albuquerque	0.572	2.438	15.831	Seattle	0.767	4.350	24.438	Tapachula	1.104	3.476	34.416	37	90.57
27	Chicago	1.042	1.933	15.220	Seattle	0.875	2.551	17.965	Iqualit	0.915	3.355	35.691	37	90.76
28	Chicago	0.884	1.870	14.609	Boston	0.767	2.729	12.752	Gander	0.791	3.152	29.736	37	88.59
29	Cleveland	0.570	2.827	13.462	Minneapolis	0.666	3.678	9.679	San Juan	0.985	3.225	31.931	37	90.70
30	Chicago	0.860	2.957	28.709	Seattle	0.861	2.515	12.638	Iqualit	0.787	4.574	16.049	36	91.50
31	Memphis	0.744	2.343	30.829	Oakland	0.954	2.652	12.000	Iqualit	0.847	4.014	20.798	37	90.24
32	Cleveland	0.751	2.541	12.769	Oakland	0.847	3.488	12.413	Iqualit	0.866	3.880	26.944	37	89.43
33	Denver	0.547	2.876	9.523	Oakland	0.893	3.395	11.470	Kotzebue	0.617	6.033	27.423	36	90.17
34	Chicago	0.902	2.198	14.752	Los Angeles	0.763	4.145	31.641	Barrow (2)	0.555	4.466	24.011	36	92.00
Ave		**0.783**	**3.735**	**21.845**		**0.846**	**4.147**	**22.947**		**0.776**	**7.375**	**28.162**		**90.16**
Max		**1.452**	**11.962**	**34.340**		**1.206**	**7.887**	**39.665**		**1.104**	**37.487**	**37.942**		

Notes:

(1) Very large Alaskan errors attributed to brief period of Ionospheric Scintillation on 30 March 2007 and May 2007 in WAAS DR 52. Maximum VPE at Fairbanks (2nd Worst site in PAN 21) was 13.298 m during PAN 21 period; VPL ratio = 0.556; VPE_95% = 1.000 m.

(2) PA site count and no. days for PAN report #34 excludes Tapachula station, which was listed in Table 1-1 but showed zero days of data collection.

(3) No 95% HPE or VPE listed for Dallas in Table 2-2 of PAN #14. As a filler, 95% HPE of station with 2nd largest max. HPE among inner WRSs (Cleveland) is listed instead.

(4) No specific explanation of large Cleveland error. Appears to be blamed on ionospheric storms during this quarter (April - June 2005). HPL "safety margin index" in Table 5-1 appears to contradict this number.

Table A2: *Horizontal* Error and Protection Level (in meters) from WAAS PAN Reports (Jan. 2004 – Sept. 2010)